Passive and iontophoretic transdermal delivery of phenobarbital: implications in paediatric therapy.

[1,2]Asma Djabri, [1]Richard H. Guy and [1,3] M. Begoña Delgado-Charro

[1] Department of Pharmacy & Pharmacology, University of Bath, Claverton Down, BA2 7AY, UK

[2] Present address: Asma Djabri: ITH Pharma, Unit 4 Premier Park, Premier Park Road, London, NW10 7NZ, UK

E- mail addresses:

Asma Djabri: asma.djabri@ithpharma.com

Richard H. Guy : R.H.Guy@bath.ac.uk

M. Begoña Delgado-Charro: B.Delgado-Charro@bath.ac.uk

[3] Corresponding author:

Department of Pharmacy & Pharmacology, University of Bath, Claverton Down, BA2 7AY, UK

Phone: +44 (0) 1225 383969

Fax: +44 (0) 1225 386114

B.Delgado-Charro@bath.ac.uk

Abstract

The objective of this investigation was to evaluate phenobarbital transdermal delivery for possible use in paediatric care. *In vitro* experiments were performed using intact pig skin and barriers from which the stratum corneum had been stripped to different extents to model the less resistant skin of premature babies. Cathodal iontophoretic delivery of phenobarbital was superior to anodal transport and optimised delivery conditions were achieved by reduction of competing co-ion presence in the drug formulation. Phenobarbital transport across intact or partially compromised skin was controlled by iontophoresis which was more efficient than passive diffusion. Across highly compromised skin, however, passive diffusion increased drastically and iontophoretic control was lost. Overall, this study demonstrates the feasibility of phenobarbital transdermal delivery for paediatric patients.

Key words: paediatric, transdermal, iontophoresis, phenobarbital, premature, tape-stripping

1. Introduction

Phenobarbital is a barbiturate drug used in the treatment of different forms of paediatric epilepsy and status epilepticus (BNF for children, 2011) being the first-line choice to control neonatal seizures (Lehr, 2005, Blume, 2009, Ouvrier, 1982). It is also used to treat neonatal abstinence syndrome both in the case of sedative-hypnotic withdrawal and as an adjunct therapy to treat opiate withdrawal symptoms (Bio, 2011, Finnegan, 2005, Osborn, 2010). Due to developmental changes in children, the pharmacokinetics of phenobarbital are highly variable in this population; doses are, therefore, titrated according to the individual's response for adequate seizure control while avoiding, at the same time, adverse effects due to supra-optimal levels (BNF for children 2011, Finnegan, 2005, Heimann, 1977, Lehr, 2005, Touw, 2000). The target therapeutic plasma concentrations are set between 40 and 180 $\mu mol.mL^{-1}$ depending on the application envisaged (Bio, 2011, Finnegan, 2005, Lehr, 2005, Touw, 2000). Heimann (1977) found that the elimination half-life of phenobarbital in mature neonates (118 ± 16 h) is significantly longer than that in infants of 2-12 months (63 ± 5h) and in children aged 2-5 years (68 ± 3h). Touw (2000) found that the elimination half-life varied between 48 and 147 h for a group of 19 term and preterm neonates. Phenobarbital clearance is slowest for newborns, increasing rapidly during the first two weeks of life and reaching a peak at 6-12 months. On the other hand, the total clearance normalized per kg body weight appears to decrease with increasing maturity (Touw, 2000, Lehr 2005). The average clearance of phenobarbital in neonates is about 4.3 $mL.h^{-1}.kg^{-1}$ (Touw, 2000) whereas, for older children, a mean value of approximately 8 $mL.h^{-1}.kg^{-1}$ is observed

65 (Botha, 1995, Heimann, 1977, Winter, 2010). Phenobarbital distribution volume
66 decreases with age and with gestational age; Touw (2000) reported a mean volume
67 of distribution of 0.71 ± 0.21 $L.kg^{-1}$ for term and preterm neonates. Heimann (1977)
68 used a two-compartmental model to describe phenobarbital kinetics in children of
69 several age groups, from term neonates up to 5 years old, and found a modest age
70 dependency for both the volume of distribution in the steady-state and the volume
71 of the central compartment; the values reported for V_{ss} ranged from 0.85 ± 0.06 to
72 0.67±0.07 $L.kg^{-1}$.

73 Phenobarbital is well absorbed orally (Winter, 2010); however, tablets are not
74 suitable for neonates and young children and the only approved oral alternative
75 described in the BNF (BNF for children, 2011) contains 38% ethanol. Regular
76 administration of this elixir may cause alcohol toxicity, especially in neonates. As
77 consequence, extemporaneous formulations, including suspensions from crushed
78 tablets, are sometimes prepared (Cober, 2007, Colquhoun-Flannery 1992). Slow
79 intravenous injections are also frequently used, but care must be taken to dilute the
80 parenteral formulation (200 $mg.mL^{-1}$ phenobarbital in 90% propylene glycol) to
81 provide suitable doses for young infants and children and to avoid accumulation of
82 the cosolvent (Allagaert, 2010, BNF for children 2011).

83 Passive transdermal delivery of phenobarbital has been suggested as an
84 alternative route of administration (Bonina, 1993). In this earlier *in vitro* study, drug
85 flux across excised skin from premature infants (29 – 35 weeks gestational age) was
86 approximately 4-fold greater (0.4 ± 0.13 $\mu g.h^{-1}.cm^{-2}$) than that (0.1 ± 0.02 $\mu g.h^{-1}.cm^{-2}$)
87 through either adult or full-term (37 – 40 weeks gestational age) skin. In general,
88 fluxes were inversely related to the gestational age of the donor. It was estimated

89 that a 25 cm^2 transdermal patch would be sufficient to provide an average steady-
90 state plasma concentration of 3.2 $mg.L^{-1}$ (14 µM) for a 1 kg neonate. However, the
91 feasibility of the approach employed may be questioned as the vehicle used in this
92 work was pure ethanol which is known to be toxic to preterm newborns when
93 absorbed across the skin from cleaning products (Harpin, 1982). Further, the total
94 skin surface area of a neonate varies between 0.03 and 0.25 m^2 depending on
95 gestational age (Touw, 2000). While there are no guidelines concerning the
96 maximum acceptable size of a transdermal patch for neonatal use, values in the
97 range of 1-10 cm^2 would be consistent with current usage in adults: for these
98 individuals, total skin area is ~ 2 m^2, while largest patches in use are in the order of
99 50 cm^2. Finally, the systemic concentration achievable (14 µM) is lower than the
100 recommended target for paediatric patients (40 – 180 µM).

101 Here, an optimised approach to the delivery of phenobarbital across both intact
102 and premature skin is proposed. Using iontophoresis as a physical enhancement
103 method, improved delivery rates of the drug are achieved compared to passive
104 diffusion suggesting that smaller patch sizes can be used to attain therapeutic
105 systemic levels. With iontophoresis, the much more water-soluble sodium salt of
106 phenobarbital is preferred eliminating the need for incorporation of co-solvents
107 (such as ethanol) in the topical formulation. The aqueous solubility of sodium
108 phenobarbital (molecular weight = 254.2 Da) is 1 g/mL, approximately 1000-fold
109 greater than that of the free acid. Intact and premature neonatal skin barriers were
110 modelled *in vitro* using pig skin, from which stratum-corneum was differentially tape-
111 stripped as previously described (Sekkat, 2004a, 2004b).
112

2. Materials and methods

2.1 Chemicals

Sodium phenobarbital (PHEN), silver wire (99.99%), silver chloride (99.999%), sodium hydroxide pellets, and NaOH 50% solution (ion chromatography eluent grade) were purchased from Sigma Aldrich (Gillingham, UK). Potassium dihydrogen phosphate, HEPES (4-(2-hydroxyethyl)-1-piperazine ethanesulfonic acid (HEPES) and sodium chloride were obtained from Acros (Geel, Belgium). Acetonitrile and hydrochloric acid were provided by Fisher Scientific (Loughborough, UK). All reagents were at least analytical grade and deionised water (resistivity ≥ 18.2 MΩ.cm, Barnsted Nanopure Diamond^{TM}, Dubuque, IA) was used for the preparation of all solutions.

2.2 Skin

Fresh pig skin was obtained from a local slaughterhouse, cleaned under cold running water, and stored in a refrigerator until the following day. Abdominal skin was dermatomed (Zimmer™ Electric Dermatome, Dover, Ohio) to a nominal thickness of 750 µm, cut into (10 x 10 cm^2) pieces, wrapped individually in Parafilm™, and then kept in a freezer (-20 °C) until use. Prior to the experiments, the skin was thawed at room temperature for 30 minutes and excess hair was cut with scissors. The large piece of skin was then cut into 4 portions. One served as representative of the intact skin barriers while the others were subjected a tape-stripping procedure to create different degrees of compromised skin. The intact barriers were characterized by transepidermal water loss (TEWL) measurements (AquaFlux AF-102,

137 Biox Systems Ltd., London, UK) of 9.0 ± 1.7 $g.m^{-2}.h^{-1}$. The three other pieces of skin
138 were repeatedly tape-stripped (2 x 2 cm, Scotch Book Tape, 3M, St. Paul, MN) to
139 progressively remove the stratum corneum. A 1.5 x 1.5 cm^2 template was affixed
140 onto the skin before the stripping procedure started to ensure the removal of
141 stratum corneum was from the same location. Periodic measurement of TEWL
142 allowed the degree of barrier compromise to be quantified and full barrier
143 impairment was defined when the removal of three consecutive tape strips did not
144 alter TEWL. The number of tape strips required to produce a fully compromised
145 barrier varied between 13 and 23. The second and third pieces of skin were tape-
146 stripped until TEWL reached values of between 20-40% and 60-80%, respectively, of
147 the TEWL recorded for the fully compromised barrier. Thus, three levels of barrier
148 function impairment were studied: 20-40% (Intermediate "less" barrier), 60-80%
149 (Intermediate "plus" barrier), and 100% (fully compromised barrier).

150 **2.3 Iontophoresis set-up**

151 Side-by-side two-compartment diffusion cells (active transport area = 0.78 cm^2,
152 volume = 3.3 mL) were used in all experiments. The skin was mounted between the
153 two chambers with the epidermal side oriented towards the cathode compartment.
154 The receptor chamber always held 154 mM sodium chloride solution (unbuffered,
155 pH ~ 6). Prior to the start of the transport study, the skin was left for 30 minutes in
156 contact with the donor vehicle without drug, and 154 mM sodium chloride in the
157 receptor chamber. The compartments were then emptied and refilled with a donor
158 solution containing sodium phenobarbital and with fresh receptor solution. Both
159 compartments were magnetically stirred (Multipoint-6 stirrer, Thermo Scientific
160 Variomag, Cole-Parmer, UK) throughout the experiment. A direct constant current of

161 0.4 mA (0.5 mA.cm^{-2}) was delivered using Ag/AgCl electrodes and a power supply
162 (KEPCO 1000M, Flushing, NY, USA). Hourly samples (0.5 mL) of the receptor phase
163 were withdrawn for analysis and replaced with fresh receptor solution. Experiments,
164 which compared phenobarbital iontophoretic delivery through different skin
165 barriers, also monitored passive permeation (same donor solution) post-current
166 termination. Separate passive diffusion controls (no current) through both intact and
167 compromised skin were also performed. The details of the experiments performed
168 are in Table 1.

169 Another series of experiments examined the effect of iontophoresis on the
170 passive permeability of intact skin to phenobarbital. Prior to the permeation study,
171 and in the absence of phenobarbital (i.e., with a donor compartment containing
172 water, pH 8.5, and receptor compartment containing unbuffered 154 mM NaCl), a
173 0.4 mA current was applied for 5 hours. At this point, the current was terminated
174 and the compartments were then emptied and refilled with a donor solution
175 containing phenobarbital and with fresh receptor solution. Passive diffusion was
176 then followed for 24 hours. To account for any effect of skin hydration during the
177 pre-iontophoresis, the same experiment was repeated without application of current
178 and with the donor and receptor compartments being filled with water and 154 mM
179 NaCl, respectively.

180 **2.4 Phenobarbital and chloride analysis**

181 Quantification of phenobarbital was performed by high performance liquid
182 chromatography with UV detection (215 nm). The method was modified from a
183 previous publication (Sekkat, 2004b) and used a Jasco HPLC system (PU-980 pump
184 with an AS-1595 autosampler, a UV-975 UV-VIS detector, and an Acclaim 120, C18

185 (150 x 4.6 mm, 5µm) reversed-phase column (Dionex, UK) which was thermostated
186 at 30 °C). The mobile phase, pumped at 1 mL.min^{-1}, consisted of phosphate buffer
187 (0.067 M KH_2PO_4) and acetonitrile (70:30) and the pH was adjusted to 6 with NaOH.

188 Chloride was analysed by ion chromatography with suppressed conductivity
189 detection (Sylvestre, 2008) using a Dionex system (Sunnyvale, CA) comprising a GP-
190 50 gradient pump, an AS-50 autosampler and thermal compartment, and an ED-50
191 electrochemical detector. The mobile phase, 35 mM NaOH, was pumped isocratically
192 (1 mL.min^{-1} flow rate) through a Dionex IonPacTM AS16 (250 x 4 mm) column
193 thermostated at 30^{o}C and connected to a Dionex ASRS Ultra II suppressor (4 mm) set
194 at a current of 90 mA.

195 **2.5 Data analysis and statistics**

196 Data analysis was performed using Graph Pad Prism V.5.00 (Graph Pad Software
197 Inc., CA, USA). Unless otherwise stated, data are presented as the mean ± standard
198 deviation. Transport fluxes were calculated as the amounts delivered during a
199 permeation period divided by the length of that period. Statistical significance was
200 set at $p < 0.05$. Comparisons made between different sets of data were assessed by
201 either a two-tailed unpaired t-test (for 2 groups) or a one-way ANOVA (for > 2
202 groups) followed by Tukey's post-test. Comparison of fluxes at different times was
203 assessed by repeated-measures ANOVA followed by Tukey's post-test.

204 The corrected transference number ($t_{COR,PHEN}$) of phenobarbital was computed
205 according to Faraday's law (Phipps, 1992):

206 $$t_{PHEN} = \frac{J_{COR,PHEN,} \cdot z \cdot F}{I}$$ Equation 1

where, $J_{COR,PHEN}$ is the corrected flux, *I* is the current intensity applied, *F* is faraday's constant, and z the absolute value of the drug valence. Transference numbers were calculated from the corrected fluxes representing those observed after 5 hours iontophoresis (J_{PHEN}) minus the passive diffusion rate 5 hours post-current termination.

3. Results and discussion

3.1 Passive diffusion across intact skin

The passive diffusion of phenobarbital from a 50 mM aqueous drug solution (pH 8.5) across (i) untreated skin, (ii) skin pre-treated with 0.4 mA current for 5 hours, and (iii) skin hydrated for 5 hours is shown in Figure 1 in terms of drug permeation as a function of time. The cumulative amounts transported (± SD) 24 hours post-drug application were: 91.7 ± 33.7, 415 ± 125, and 222 ± 35.5 $nmol.cm^{-2}$ for untreated, pre-iontophoresed, and pre-hydrated skin, respectively. Passive diffusion across pre-iontophoresed skin was significantly higher than through untreated ($p < 0.01$) and pre-hydrated ($p < 0.05$) skin. Increased permeability of skin previously exposed to direct current has been previously reported (Green, 1992).

3.2 Iontophoretic delivery across intact skin

The first donor solution tested was 50 mM sodium phenobarbital in water (pH 8.5) where the drug (pK_a = 7.3) (Merk Index, 2006) was ~93 % ionised. Cathodal iontophoresis resulted in drug delivery that was 385-fold higher than passive diffusion (Figure 2). After only 1 hour of current application, the phenobarbital flux was 222 ± 94.4 $nmol.h^{-1}$ increasing to 387 ± 57.2 $nmol.h^{-1}$ by 3 hours. At the end of the experiment (5 h), the flux was 341 ± 64.5 $nmol.h^{-1}$.

A second series of iontophoresis experiments compared anodal *versus* cathodal delivery of phenobarbital at pH 7.4 where phenobarbital exists in essentially equal concentrations of the ionized and unionized forms. The former, of course, can be delivered from the cathode by electro-repulsion, while the latter may be transported from the anode by electro-osmosis. A donor concentration of 15 mM was used because of phenobarbital's lower solubility at this pH. Chloride ions are required to ensure adequate electrochemistry at the anode, and 50 mM NaCl was therefore added to both the cathodal and anodal solutions. Cathodal iontophoresis (Figure 3) was much more efficient than anodal. When the contribution of passive diffusion was taken into account, the corrected cathodal and anodal fluxes at 5 hours were 42.4 ± 13.3 and 7.1 ± 3.8 $nmol.h^{-1}$, respectively. These results are in good agreement with previous data (e.g., for 5-fluorouracil (Merino, 1999) and for phenytoin (Leboulanger,2004)) which showed that electromigration is a much more efficient transport mechanism than electroosmosis. The reduced cathodal delivery observed here relative to that observed at pH 8.5 is explained by the lower concentration of ionized drug employed, decreasing from 46.3 mM (~93 % of 50 mM) to 7.5 mM (~50% of 15 mM) and by the presence of 50 mM competing chloride ions in the pH 7.4 experiment.

The effect of co-ion competition on cathodal delivery by electro-repulsion was then investigated. In an initial experiment, a 15 mM PHEN solution, the pH of which had been adjusted to 7.4 with HCl was used, resulting in introduction of Cl^- at a concentration of approximately 6 mM. As this represents a lower level of chloride ions compared to the earlier experiment, an increase in t_{PHEN} and PHEN flux might have been expected. However, the concentration of competing chloride increases

254 above the initial 6 mM during the experiment because of the gradual release of Cl^-
255 from the cathode as the electrochemistry reduces AgCl to Ag (Figure 4). This implies
256 that transport number of the drug would decrease as the experiment proceeds.

257 A subsequent experiment attempted to mitigate the impact of chloride
258 accumulation on the cathodal flux of PHEN by refreshing the donor solution every
259 hour. In a related experiment, 10 mM HEPES was employed as a buffer for the 15
260 mM sodium phenobarbital donor solution. This provided good buffer capacity
261 without requiring any adjustment to pH 7.4 with HCl (thereby avoiding the
262 introduction of extra chloride ions). Again, to counter the build-up of chloride ions
263 released from the electrode, the donor solution was refreshed hourly. It was
264 calculated that Cl^- release from the cathode would contribute (in the diffusion cells
265 used) a concentration of 4.5 mM for every hour of 0.4 mA current applied. Figure 4
266 illustrates the anticipated evolution of chloride concentration in the donor solution
267 as a function of time under the experimental conditions employed. The predicted
268 values agree closely with those measured experimentally by ion chromatography.

269 The PHEN fluxes were inversely related to the Cl^- concentration present in the
270 donor solution after 5 hours of current application. The greater the co-ion
271 competition with PHEN, the lower the drug transport (Figure 4). Chloride
272 accumulation in the cathodal chamber plays a key role in the iontophoretic delivery
273 of negatively-charged drugs as previously demonstrated for dexamethasone
274 phosphate (Sylvestre, J.P., 2008a. 2008b) and needs careful optimization.

275 The transport number of phenobarbital (t_{PHEN}) was linearly proportional ($r^2 \approx$
276 0.80) to the drug's molar fraction in the vehicle (Figure 5). Following the principles
277 demonstrated by Mudry et al. (2006) for cation electrotransport, and assuming their

278 validity for the anionic PHEN, the maximum transport number of the drug at pH 7.4,
279 i.e., in the absence of competing co-ions, is estimated to be 0.035 (determined by
280 substitution of X_{PHEN}=1 in the linear regression equation given in Figure 5).

281 **3.3 Permeation across compromised skin**

282 The objective of this part of study was to examine the permeation of
283 phenobarbital across barriers representative of those found in premature neonates
284 whose stratum corneum may be absent or not fully developed. Three impaired levels
285 of barrier function were evaluated against intact skin for passive as well as
286 iontophoretic delivery of the drug. The average TEWL measurements ($g.m^{-2}.h^{-1}$)
287 across the different skin barriers were as follows: 11 ± 1, 44 ± 10, 114 ± 20, and 158 ±
288 25, respectively, for intact, intermediate "less"(20 – 40 %), intermediate "plus" (60 –
289 80 %), and fully compromised skin. The TEWL values were significantly higher than
290 those reported in previous studies, which validated the usefulness of serially
291 stripped pig skin as a model for that of the developing neonate and subsequently
292 employed the approach to predict the transdermal permeation of phenobarbital,
293 caffeine, and lidocaine (Sekkat 2004a, 2004b). The discrepancy is between a factor of
294 two and four and is probably due to the different TEWL devices employed in the two
295 studies (i.e., the study closed-chamber evaporimeter (AquaFlux AF102, Biox) used
296 here versus an open-chamber instrument (EP1, Servomed) used before (Farahmand,
297 2009, Imhof 2009). Other factors may have played a part, such as the number of
298 tape-strips used to remove the stratum corneum, and the pressure with which the
299 tapes were applied (Escobar-Chavez, 2008, Rubio et al., 2011).

300 Passive diffusion of phenobarbital increased dramatically as the stratum
301 corneum was progressively compromised (Figure 6). The flux at 5 hours through

intact skin was only 0.9 ± 0.2 nmol.h^{-1}, but increased to 810 ± 251 nmol.h^{-1} for fully compromised skin. Transport through barriers with intermediate levels of impairment levels fell between these two extremes: 31 ± 12 nmol.h^{-1} and 561 ± 179 nmol.h^{-1} for 20-40 % and 60-80 % of barrier disruption, respectively.

Previously, a similar phenobarbital permeation rate across intact full-thickness pig ear skin was measured when the drug was delivered from a saturated solution of the unionised drug (4.3 mM) at pH 5 (Sekkat, 2004b). Permeation across fully compromised skin was ~30 times higher than that through the intact barrier. In contrast, the enhancement factor observed in this work was more than 900-fold due, at least in part, to the fact that most of the drug was ionised (~3.7 mM unionized) and hence in a less favourable form for passive permeation. With progressive removal of the stratum corneum, the ionised and neutral forms of phenobarbital permeated through the less-resistant skin barrier at much higher rates. Similar behaviour has been seen for 5-fluorouracil (Fang, 2004), with removal of the stratum corneum leading to an increase in passive diffusion from < 0.03 µmol.cm^{-2} in 6 hours to approximately 17 µmol.cm^{-2} a difference of more than 550-fold.

Figure 6 summarizes the iontophoretic delivery of phenobarbital through compromised skin barriers. The fluxes measured during 5 hours of iontophoresis (0.4 mA) application followed by 5 hours of passive diffusion are shown. Table 2 presents the fluxes during the last hour of the permeation studies. The iontophoretic fluxes observed increased with the level of skin impairment but complete removal of the stratum corneum only resulted in a 3.6-fold enhancement relative to intact skin (Table 2). When the contribution of passive diffusion is taken into account, the corrected iontophoretic fluxes, and the corresponding t_{PHEN}, are very similar for all

skin barriers tested (Table 2). In fact, no significant differences were found between these values. It follows that while iontophoretic flux remained constant and independent of the skin barrier function, passive diffusion increased remarkably as the skin was progressively compromised and eventually overshadowed any benefits from iontophoresis. Qualitatively, these results are consistent with those reported for lidocaine hydrochloride (Sekkat, 2004b), for which the total iontophoretic delivery was practically the same across intact (1.8 ± 0.5 $mg.cm^{-2}$) and tape-stripped skin (1.9±0.3 $mg.cm^{-2}$). In contrast, the passive permeability of lidocaine HCL increased from $7x10^{-4}$ ± $4x10^{-4}$ $mg.cm^{-2}$ across intact skin to 0.1±0.07 $mg.cm^{-2}$ through a fully tape-stripped barrier. Quantitatively, however, the difference between the behaviour of lidocaine and phenobarbital is important. In the case of lidocaine, the passive diffusion of the drug even across fully-compromised skin is still an order of magnitude smaller than iontophoretic delivery; electrotransport can be used, therefore, to control drug input independent of the status of skin barrier function. For phenobarbital, on the other hand, passive transport increases significantly with progressive derangement of the barrier, ultimately overwhelming iontophoretic delivery, which is no longer able to exercise control over the absorption of the drug when the stratum corneum has been compromised.

Finally, a summary of the passive and iontophoretic transport of phenobarbital as a function of TEWL (reflecting barriers of varying competence) is shown in Figure 7. The slopes of the linear regressions through the passive and iontophoretic fluxes are not significantly different. This emphasizes the point made above that, once the function of the stratum corneum has been undermined (>50%), the passive transport

of phenobarbital exceeds that due to iontophoresis and dominates the transdermal delivery of the drug.

3.4 Feasibility of phenobarbital transdermal delivery

Phenobarbital is used for different purposes in neonatal and paediatric patients. Examination of the doses used for different indications (BNF for children 2011, Bio, 2011; Finnegan, 2005; Osborn, 2010) quickly reveals that the transdermal route would not provide the initially large doses required to treat status epilepticus (20 $mg.kg^{-1}$ for neonates) or the loading doses required for epilepsy and neonatal abstinence syndrome. However, the maintenance doses for status epilepticus are much lower: 2.5-5 $mg.kg^{-1}$ once or twice a day for both neonates and children aged 1 month to 12 years (BNF for children 2011). For epilepsy, the maintenance doses are 2.5-5 $mg.kg^{-1}.day^{-1}$ and up to 2.5-8 $mg.kg^{-1}.day^{-1}$ for neonates and children (1 month-12 years) respectively, (BNF for children 2011). The maintenance doses recommended for treating neonatal withdrawal symptoms fall in the range 2-10 $mg.kg^{-1}.day^{-1}$ (Bio, 2011; Finnegan, 2005; Osborn, 2010). The phenobarbital doses required for any of the indications mentioned in children older than 12 years are too large for transdermal administration.

Table 3 calculates the passive and iontophoretic patch sizes required to deliver maintenance doses between 2 and 10 $mg.kg^{-1}.day^{-1}$ (0.3 to 1.6 $\mu mol.kg^{-1}.h^{-1}$) i.e., amounts spanning the three potential applications of phenobarbital discussed above. The fluxes used in these calculations were those measured when the donor solution was 50 mM of drug in water at pH 8.5.

Assuming a quantitative *in vitro-in vivo* correlation, transdermal delivery of phenobarbital to neonates (including premature and full-term) appears feasible.

373 Indeed, passive would be sufficient for premature neonates with significantly
374 immature skin. However, as the skin barrier matures, iontophoresis would become
375 progressively more effective in providing desirable rates of delivery while keeping
376 patch size reasonable (Table 3). For safety reasons, and the variable degree of barrier
377 immaturity in the premature neonate, transdermal patches with rate-limiting
378 membranes may be preferable, to ensure rate-control and to avoid potential
379 toxicity. A key challenge with premature neonates is to compensate the rate of drug
380 delivery for the degree of barrier maturation.

381 Premature neonates of only 23-25 weeks gestational age may require more
382 than 4 weeks to develop a full functional stratum corneum (Kalia, 1998); whereas
383 those born at 32 weeks of more have a barrier function that is close to fully
384 functional. To treat this "moving target" would require passive patches in a variety of
385 sizes (and even designs, e.g., rate-controlling versus matrix); alternatively
386 iontophoresis might prove more useful in that the intensity and duration of current
387 can be "tuned" to provide the required drug input. This flexibility in dosage form
388 design and operation would rely, of course, on the application of TEWL
389 measurements to pinpoint barrier function status in the patient (Fluhr, 2006, Levin,
390 2005).

391 Table 3 also shows that iontophoresis may deliver therapeutic amounts of
392 phenobarbital to infants of 1 month or more to young children. For older children,
393 however, phenobarbital transdermal delivery may not be useful because the
394 requisite patch area becomes too large. For example, the patch sizes required to
395 deliver 2-10 $mg.kg^{-1}.day^{-1}$ would be 4-20 cm^2, 6-32 cm^2, and 12-64 cm^2 for paediatric
396 patients weighing 3, 5 and a 10 kg, respectively.

Ultimately, *in vivo* studies will be required to demonstrate that the *in vitro-in vivo* correlation assumed is valid and to examine the effect of current application and other formulation variables (such as pH) on the skin of infants and premature neonates.

4. Conclusions

This study demonstrated that cathodal iontophoresis of phenobarbital through intact skin is more efficient than anodal iontophoresis and passive diffusion. Competition from anions present in the donor formulation must be minimized to optimize phenobarbital delivery. The results suggest that both passive and iontophoretic delivery of this drug to premature neonatal and paediatric patients may, in some circumstances, be feasible and attractive. Of course, the costs associated with the development and use of such new transdermal systems must be carefully balanced against their potential to provide an improved and better-tolerated therapy.

Acknowledgments

A. Djabri is grateful to the Algerian Government for sponsoring her PhD.

415 **References**

416 Allagaert, K. et al., 2010. Prospective assessment of short-term propylene glycol
417 tolerance in neonates. Arch. Dis. Child. 95, 1054-1058.

418 Bio, L. L. et al., 2011. Update on the pharmacological management of neonatal
419 abstinence syndrome. J. Perinatol. 31, 692-701.

420 Blume et al., 2009. Neonatal seizures: treatment and treatment variability in 31
421 United States pediatric hospitals. J. Child. Neurol. 24, 148-154.

422 BNF for children, 2010-2011. BMJ group, Pharmaceutical Press, and RCPCH
423 Publications Ltd. London.

424 Bonina, F.P., et al., 1993. In-vitro percutaneous-absorption evaluation of
425 phenobarbital through hairless mouse, adult and premature human skin. Int. J.
426 Pharm. 98, 93-99.

427 Botha, J.H. et al., 1995. Determination of phenobarbitone population clearance
428 values for south african children. Eur. J. Clin. Pharmacol. 48, 381-383.

429 Cober, M.P., Johnson, C.E. 2007. Stability of an extemporaneously prepared
430 alcohol-free phenobarbital suspension. Am. J. Health-Syst. Pharm. 64, 644-646.

431 Colquhoun-Flannery, W., Wheeler, R. 1992. Treating neonatal jaundice with
432 phenobarbitone: the inadvertent administration of significant doses of ethyl-alcohol.
433 Arch. Dis. Child. 67, 152-152.

434 Escobar-Chavez, J.J., et al., 2008. The tape-stripping technique as a method for
435 drug quantification in skin. J. Pharm. Pharm. Sci. 11, 104-130.

436 Fang, J.Y., et al., 2004. Transdermal iontophoresis of 5-fluorouracil combined
437 with electroporation and laser treatment. Int. J. Pharm. 270, 241-249.

438 Farahmand, L. et al., 2009. Measuring transepidermal water loss: a comparative
439 in vivo study of condenser-chamber, unventilated-chamber and open-chamber
440 systems. Skin Res. Tech. 15, 392-398.

441 Finnegan, L. Kandall, S.R. 2005, Neonatal abstinence syndromes, in: Yaffe, S.J.,
442 Aranda, J.V. (Eds), Neonatal and pediatric pharmacology: therapeutic principles in
443 practice, third ed., Lippincott Williams & Wilkins, Philadelphia; London, pp. 848-860.

444 Fluhr, J.W., et al., 2006. Transepidermal water loss reflects permeability barrier
445 status: validation in human and rodent in vivo and ex vivo models. Exp. Dermatol. 15,
446 483-492.

447 Green, P., et al., 1992. In vitro and in vivo iontophoresis of a tripeptide across
448 nude rat skin. J. Control. Release. 20, 209-217.

449 Harpin, V., Rutter, N., 1982. Percutaneous alcohol absorption and skin necrosis
450 in a preterm infant. Arch. Dis. Child. 57, 477-479.

451 Heimann, G., Gladtke, E.,1977. Pharmacokinetics of pehnobarbital in childhood.
452 Europ. J. Clin. Pharmacol. 12, 305-310.

453 Kalia, Y.N., Nonato, L.B., Hund C.H., Guy, R.H., 1998. Development of skin
454 barrier function in premature infants. J. Invest. Dermatol. 111, 320-326.

455 Imhof, R.E., et al., 2009. Closed-chamber transepidermal water loss
456 measurement: microclimate, calibration and performance. Int. J. Cosmet. Sci., 31,
457 97-118.

458 Leboulanger, B., et al. 2004. Non-invasive monitoring of phenytoin by reverse
459 iontophoresis. Eur. J. Pharm. Sci., 22, 427-433.

460 Lehr, V.T. et al., 2005. Anticonvulsants, in: Yaffe, S.J., Aranda, J.V. (Eds),
461 Neonatal and pediatric pharmacology: therapeutic principles in practice, third ed.,
462 Lippincott Williams & Wilkins, Philadelphia; London, pp. 504-519.

463 Levin, J., and Maibach H. 2005. The correlation between transepidermal water
464 loss and percutaneous absorption: An overview. J. Control. Release, 103, 291-299.

465 The Merck Index, 2006. 14th Ed. Merck & Co. Inc. Whitehouse Station, NJ, USA.

466 Merino, V., et al., 1999. Electrorepulsion versus electroosmosis: effect of pH on
467 the iontophoretic flux of 5-fluorouracil. Pharm. Res. 16, 758-761.

468 Mudry, B., et al., 2006. Prediction of iontophoretic transport across the skin. J.
469 Control. Release. 111, 362-367.

470 Osborn D.A. et al., 2010. Sedatives for opiate withdrawal in newborn infants.
471 The Cochrane Library, 10, 1-44.

472 Ouvrier, R.A., Goldsmith, R., Hey, E., 1982.Phenobarbitone dosage in neonatal
473 convulsions. Arch. Dis. Child. 57, 653-657.

474 Phipps, J.B. and Gyory, J.R. 1992. Transdermal ion migration. Adv. Drug. Deliv.
475 Rev. 9, 137-176.

476 Rubio et al., 2011. Barrier function of intact and impaired skin: percutaneous
477 penetration of caffeine and salicylic acid. Int. J. Dermatol. 50, 881-889.

478 Sekkat, N., Kalia, Y.N., Guy, R.H., 2004a. Development of an in vitro model for
479 premature neonatal skin: biophysical characterization using transepidermal water
480 loss. J. Pharm. Sci. 93, 2936-2940.

481 Sekkat, N., Kalia, Y.N., Guy, R.H., 2004b. Porcine ear skin as a model for the
482 assessment of transdermal drug delivery to premature neonates. Pharm. Res. 21,
483 1390-1397.

484 Sylvestre, J.P., et al., 2008a. Iontophoresis of dexamethasone phosphate:
485 competition with chloride ions. J. Control. Release, 131, 41-46.

486 Sylvestre, J.P., et al., 2008b. In vitro optimization of dexamethasone phosphate
487 delivery by iontophoresis. Phys. Ther., 88, 1177-1187.

488 Touw, D.J., et al., 2000. Clinical pharmacokinetics of phenobarbital in neonates.
489 Eur. J. Pharm. Sci. 12, 111-116.

490 Winter M.E.,2010. Basic clinical pharmacokinetics, fifth ed. Lippincott William &
491 Wilkins, Philadelphia.

492

493

494 **Table 1:** Experiments performed to characterise phenobarbital transdermal

495 delivery through intact, pretreated and impaired skin.

Skin barrier	Donor	PHEN (mM)	Experiment settings and duration	n
Intact	Water (pH 8.5)	50	(1) Cathodal iontophoresis (5h), then passive diffusion (5h)	3
			Passive diffusion (24h)	3
	50 mM NaCl (pH 7.4)	15	(2) Cathodal iontophoresis (5h)	4
			Anodal iontophoresis (5h)	4
			Passive diffusion (24h)	6
	Water (pH 7.4)	15	(3) Cathodal iontophoresis (5h)	6
			(4) Cathodal iontophoresis (5h). Donor solution exchanged hourly	5
	10 mM HEPES (pH 7.4)	15	(5) Cathodal iontophoresis (5h). Donor solution exchanged hourly	5
Pre-treated	Water (pH 8.5)	50	Pre-treatment: 0.4 mA for 5 h followed by passive diffusion (24h)	4
			Pre-treatment: hydration for 5 h followed by passive diffusion (24h)	
Impaired: 20-40 % 60-80 % 100 %	Water (pH 8.5)	50	Cathodal iontophoresis (5h), then passive diffusion (5h)	3-5
			Passive diffusion (24h)	3-5

496

497

498 **Table 2:** Fluxes of phenobarbital (µmol.h^{-1}, mean ± SD), through differentially-
499 impaired skin barriers, after 5 hours of iontophoresis, and after a further 5 hours of
500 passive diffusion post-current application. The corrected values ($J_{COR,PHEN}$) are the
501 differences between the measurements in the first two columns and are used to
502 calculate the transport number (t_{PHEN}) shown.
503

Skin barrier	Iontophoresis J_{PHEN}	Passive post-iontophoresis	Corrected $J_{COR,PHEN}$	10^2 x t_{PHEN}
Intact	0.34 ± 0.06	0.05 ± 0.01	0.30 ± 0.07	2.0 ± 0.4
Intermediate “less”	0.60 ± 0.09	0.24 ± 0.08	0.35 ± 0.08	2.4 ± 0.5
Intermediate “plus”	0.94 ± 0.27	0.63 ± 0.31	0.31 ± 0.09	2.1 ± 0.6
Fully compromised	1.23 ± 0.32	0.92 ± 0.25	0.31 ± 0.08	2.1 ± 0.5

504
505
506
507
508

509 **Table 3:** Estimated patch sizes required to deliver maintenance doses of
510 phenobarbital assuming that the *in vitro* fluxes determined in this work are reflective
511 of those achievable *in vivo*.

512

Skin type:	Intact	Intermediate "less"	Intermediate "plus"	Fully compromised
Passive				
In vitro flux (µmol.h^{-1}.cm^{-2}) [a]	*Negligible*	*0.1 ± 0.02*	*0.8 ± 0.2*	*1.1 ± 0.4*
Patch size required (cm^2.kg^{-1})		*3 – 16*	*0.4 – 2*	*0.3 – 1.5*
Iontophoresis (0.5 mA.cm^{-2})				
In vitro flux (µmol.h^{-1}.cm^{-2}) [a]	0.5 ± 0.1	0.7 ± 0.1	1.2 ± 0.4	1.5 ± 0.4
Area per electrode (cm^2.kg^{-1})	0.6 – 3.2	0.4 – 2.3	0.25 – 1.3	0.2 – 1.1
Total patch size (cm^2.kg^{-1}) [b]	1.2 – 6.4	0.8 – 4.6	0.5 – 2.6	0.4 – 2.2

513

514 [a] Fluxes are the average values measured after 2 – 5 hours of iontophoresis (0.5 mA.cm^{-2}) or
515 passive diffusion.

516 [b] Assuming that the areas occupied by the anodal and cathodal electrode formulations are
517 the same.

518

519

Figure legends

Figure 1: Passive diffusion of phenobarbital through intact pig skin. Pre-treatment either involved 5 hours direct current at 0.4 mA or 5 hours hydration without current. Phenobarbital was not present in the pre-treatment periods. Data are represented as the mean ± SD.

Figure 2: Passive and iontophoretic transdermal fluxes (mean ± SD) of phenobarbital after 5 hours from a 50 mM drug solution.

Figure 3: Anodal and cathodal iontophoresis of phenobarbital when delivered from a 15 mM drug solution at pH 7.4. The passive diffusion control is also shown. Data points are represented as mean ± SD.

Figure 4: *Left panel*: Estimated donor concentration of chloride ions (dashed lines) and the corresponding measurements (symbols, mean ± SD) for experiments 3 (▲), 4 (□), and 5 (●) as indicated in Table 1. *Right panel:* Cathodal delivery of phenobarbital from different donor solutions (pH 7.4) containing various amounts of competing co-ions (experiments 2-5 in Table 1). The flux values (mean ± SD) were determined after 5 hours of iontophoresis (0.4 mA).

Figure 5: Transport number of phenobarbital (t_{PHEN}, mean ± SD) as a function of molar fraction (X_{PHEN}). Values of the latter parameter were calculated from the concentrations of phenobarbital, HEPES, and chloride. The sources of Cl^- included NaCl (used as background electrolyte), HCl (used to adjust the donor solution pH), and the electrode electrochemical reaction. Data expressed by the same symbol and number represent the experimental condition as identified in Table 1. The dashed line is the linear regression through all data points except those obtained with HEPES: $t_{PHEN} = 0.002\ (\pm 0.001) + 0.033\ (\pm 0.002)\ X_{PHEN}$, ($r^2 > 0.8$).

Figure 6: Passive (left panel) and iontophoretic (right panel) transport (mean ± SD) of phenobarbital delivered from a 50 mM drug solution through intact and compromised skin barriers. The right panel also shows the passive diffusion of phenobarbital post-current termination at 5 hours.

Figure 7: Total passive and iontophoretic fluxes of phenobarbital as a function of TEWL across skin barriers of different competencies. Open symbols refer to passive diffusion alone; filled symbols reflect the total drug flux when an iontophoretic current is applied. Intact, intermediate "less" (20–40 %), intermediate "plus" (60–80 %) and fully compromised skin barriers are respectively symbolized by diamonds, triangles, circles, and squares. Linear regressions through the passive and iontophoretic results were: $J_{Passive} = -156\ (\pm 97) + 8.3(\pm 1.1) \bullet TEW$ and $J_{ionto} = 372\ (\pm 101) + 7.0(\pm 0.9) \bullet TEWL$, with r^2 values of 0.85 and 0.82, respectively.

Figure 1

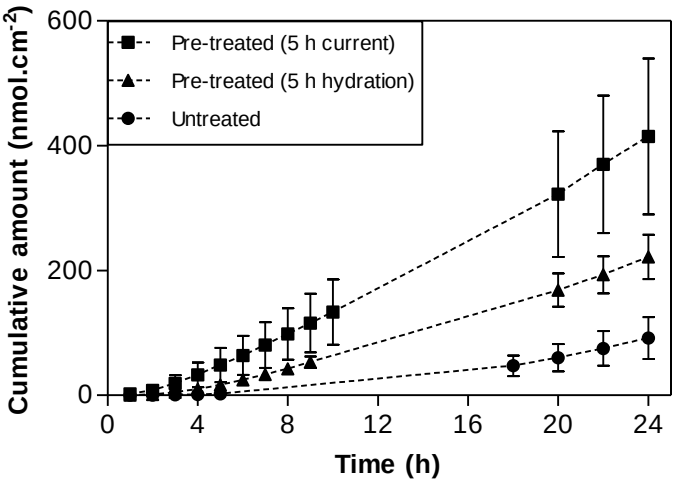
Pre-treated (5 h current)
Pre-treated (5 h hydration)
Untreated
Cumulative amount (nmol.cm-2)
Time (h)
0
200
400
600
0
4
8
12
16
20
24

Figure 2

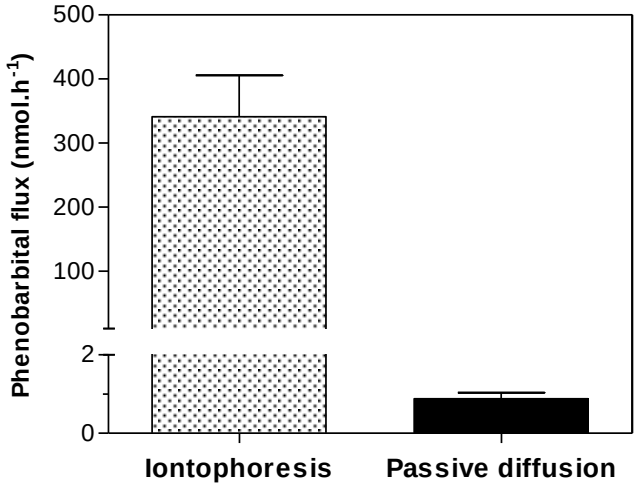
Phenobarbital flux (nmol.h-1)
500
400
300
200
100
2
0
Iontophoresis
Passive diffusion

Figure 3

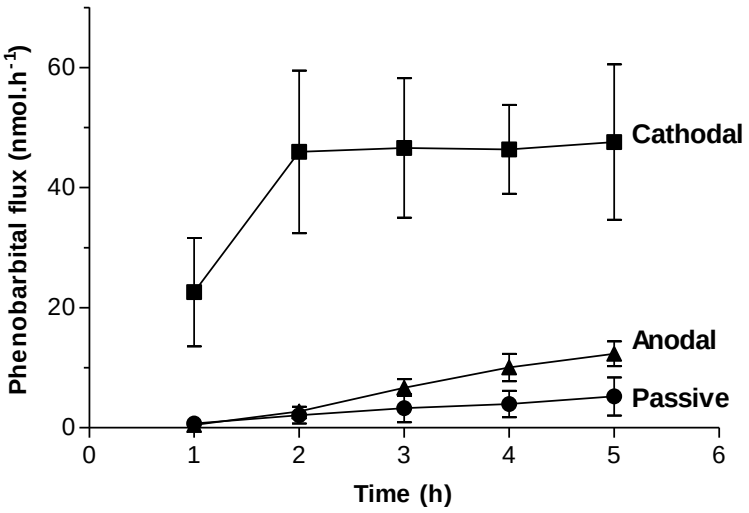
Phenobarbital flux (nmol.h-1)
60
40
20
0
0
1
2
3
4
5
6
Time (h)
Cathodal
Anodal
Passive

Figure 4

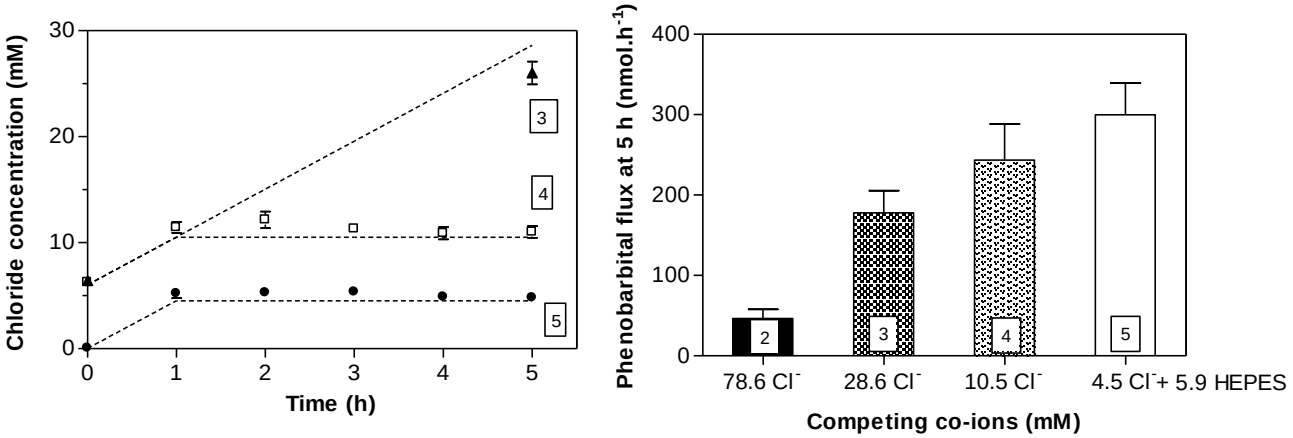
Chloride concentration (mM)
Time (h)
3
4
5
Phenobarbital flux at 5 h (nmol.h-1)
Competing co-ions (mM)
78.6 Cl-
28.6 Cl-
10.5 Cl-
4.5 Cl-+ 5.9 HEPES
2
3
4
5

Figure 5

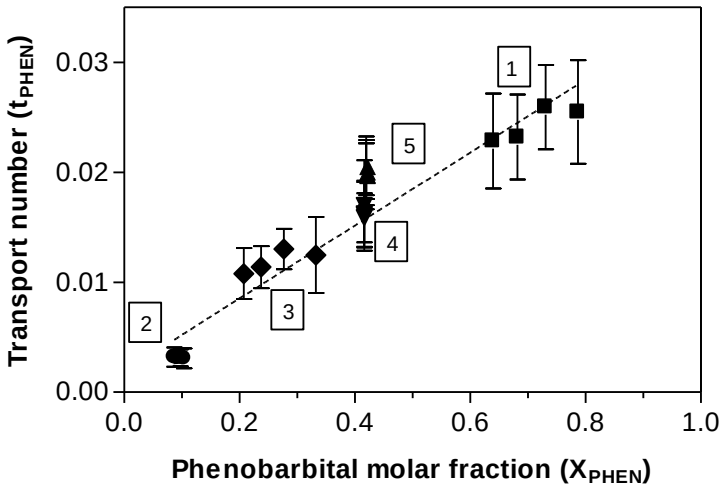
Transport number (t_{PHEN})
0.00
0.01
0.02
0.03
0.0
0.2
0.4
0.6
0.8
1.0
Phenobarbital molar fraction (X_{PHEN})
1
2
3
4
5

Figure 6

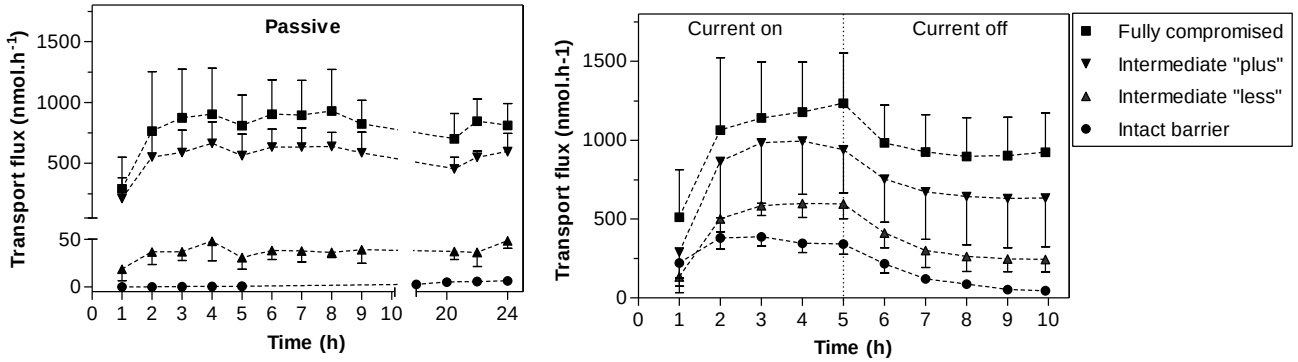
Passive
Transport flux (nmol.h-1)
1500
1000
500
50
0
0 1 2 3 4 5 6 7 8 9 10 20 24
Time (h)
Current on
Current off
Transport flux (nmol.h-1)
1500
1000
500
0
0 1 2 3 4 5 6 7 8 9 10
Time (h)
Fully compromised
Intermediate "plus"
Intermediate "less"
Intact barrier

Figure 7

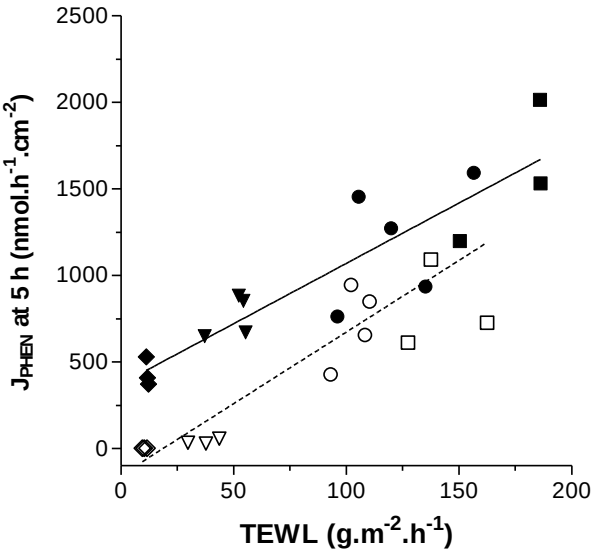
2500
2000
1500
1000
500
0
0
50
100
150
200
J_PHEN at 5 h (nmol.h-1.cm-2)
TEWL (g.m-2.h-1)

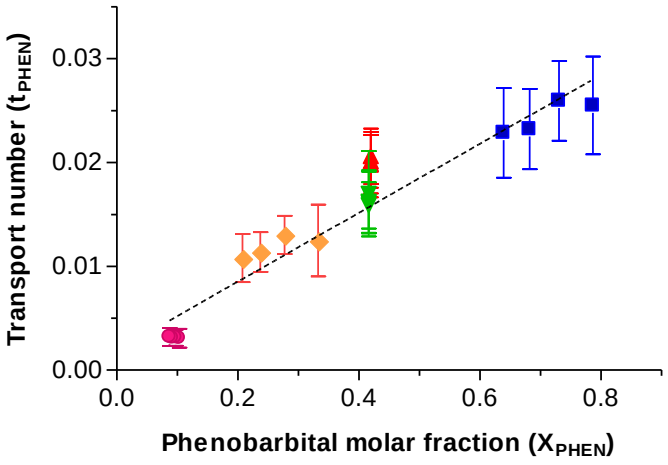
Transport number (t_{PHEN})
0.00
0.01
0.02
0.03
0.0
0.2
0.4
0.6
0.8
Phenobarbital molar fraction (X_{PHEN})

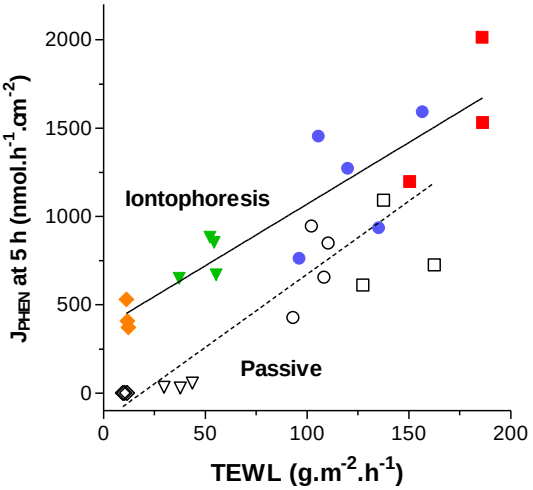
J_{PHEN} at 5 h (nmol.h^{-1}.cm^{-2})
0
500
1000
1500
2000
0
50
100
150
200
TEWL (g.m^{-2}.h^{-1})
Iontophoresis
Passive